Estimation of Plasma Emission Transition Using Hidden Markov Model*)

Shota NAKAGAWA[1)], Teruhisa HOCHIN[1,2)], Hiroki NOMIYA[1)] and Hideya NAKANISHI[2)]

[1)]*Kyoto Institute of Technology, Kyoto 606-8585, Japan*

[2)]*National Institute for Fusion Science, Toki 509-5292, Japan*

(Received 27 December 2017 / Accepted 8 August 2018)

This study proposes a method for estimating plasma-emission transitions from plasma-emission videos using a hidden Markov model (HMM). The proposed method retrieves similar videos and learns model parameters from them. The plasma-emission characteristics that we have employed are color, brightness, position, shape, and the speed at which the brightness of a plasma emissions changes. Multiple HMMs based on these plasma-emission characteristics are employed to represent the plasma-emission patterns. The anticipated plasma-emission transitions are estimated using state-transition probabilities from the generated model. Experimental results are used to confirm that the proposed methods are effective in identifying similar plasma videos and estimating probable future states of the plasma.

Keywords: hidden Markov model, video, plasma, similarity, estimation

DOI: 10.1585/pfr.13.3405117

1. Introduction

High-temperature plasma experiments are being conducted at the National Institute for Fusion Science (NIFS) [1]. During these experiments, emission is observed when the plasma reaches a sufficiently high temperature. The plasma emissions are recorded as videos and stored in disk storage at NIFS [2].

The future emission states of plasmas must be estimated to adjust experimental parameters for maintaining the plasma and making emergency stops to avoid the destruction of devices. The durations of the plasma videos range from a few seconds to one hour and more than 100,000 stored videos are available. Predicting emission patterns from past data is difficult because it takes time to manually analyze numerous videos; therefore, a system must be developed to retrieve videos from past experiments that exhibit similar characteristics and use them to determine the probabilities of future emissions.

The hidden Markov model (HMM) [3] is widely used to analyze time-series data [4, 5], particularly in the field of speech recognition, and is currently being used in other fields as well.

A method to use plasma videos to determine the probability of future plasma emissions is proposed herein, and the effectiveness of the proposed method is confirmed. The feature values of plasma videos are defined; then, an HMM is used to classify the plasma videos based on their similarities. Plasma-emission models are then generated from similar videos to determine the emission patterns. Finally, the effectiveness of the proposed method is verified via an experiment.

The remainder of this paper is organized as follows. Section 2 provides an overview of this research. Section 3 describes the related study, and Section 4 proposes our method. Section 5 describes the experiment, Section 6 discusses the results, and Section 7 concludes the study.

2. Overview of the Estimation Model

2.1 Plasma-emission videos

Plasma emission frequently occurs during high-temperature plasma experiments conducted at NIFS [1]. Video recordings of the plasma emissions are stored on disk storage at NIFS in the MPEG-1 format, with a frame rate of 29.97 frames/s. The width and height of a frame are 352×240 pixels. The durations of the videos vary, but most comprise approximately two hundred frames ($\sim$7 s).

2.2 Overview of the plasma-emission model

The procedures used to construct our plasma-emission model are as follows. First, 148 videos are prepared. Second, the videos are divided into *segments* that comprise multiple frames. For each *segment*, feature values are calculated. The videos are then categorized into 23 groups using HMM trained on the test videos. Then, the HMM parameters are determined from the *segments* in each group. Multiple HMMs are prepared by this procedure. Finally, for a prediction target video, the fitness to multiple HMMs is calculated. Then, the model representing the target video is selected.

author's e-mail: m7622031@edu.kit.ac.jp

*) This article is based on the presentation at the 26th International Toki Conference (ITC26).

3. Related Study

3.1 Visual criteria for plasma videos

Evaluation criteria to determine the similarities among plasma videos have been proposed in reference [6, 7]:

Cri. 1: Position of a bright spot
Cri. 2: Amount of movement of a bright spot
Cri. 3: Expansion and contraction of a bright spot
Cri. 4: Speed of brightness transition
Cri. 5: Amount of brightness transition
Cri. 6: Color
Cri. 7: Amount of color transition

Some researchers in fusion science consider these features to be physically significant characteristics of plasma-emission phenomena [6, 7].

3.2 Frame-hashing method

A fast-detection method for querying streaming videos was proposed in reference [8]. The original frame-hashing method divides a frame into 4×4 blocks. The luminosity of each block is averaged and binarized using the mean luminosity of the frame. Thus, binary digits can be obtained for each frame, and this constitutes the "hash value" of a frame. The hash value can then be used to detect matching scenes in streaming videos.

In this study, the frame-hashing method is used to divide a video into *segments*. A frame is divided into 16×16 blocks for more accurate division. A *segment* is defined as a series of frames exhibiting similar hash values. Figure 1 shows sample frames in both same and different *segments*. Each column of frames corresponds to a different *segment*. The upper row is the first frame of a *segment*. In Fig. 1, the next frame after the lower frame of a) is the upper frame of b), and a similar pattern follows for columns b) and c). The lower frame of a) is noticeably different from the upper frame of b), even though these frames are adjacent to each other in the time series. It can thus be seen that frames are successfully divides frames into *segments*, each of which contains similar frames.

3.3 HMM

An HMM is a generative probabilistic model, in which a sequence of observable variables is generated by a sequence of internal hidden states. An HMM is based on two conditional-independence assumptions: 1) the t^{th} hidden variable, Q_t, given the $(t-1)^{th}$ hidden variable, is independent of the previous variables, and 2) the t^{th} observation, O_t, given the t^{th} hidden variable, is independent of the other variables. These assumptions are qualitively represented by Eqs. (1) and (2), respectively:

$$P(Q_t|Q_{t-1}, O_{t-1}, \ldots, Q_1, O_1) = P(Q_t|Q_{t-1}). \quad (1)$$

$$P(O_t|Q_T, O_T, \ldots, Q_t, \ldots, Q_1, O_1) = P(O_t|Q_t). \quad (2)$$

Here, Q_t is a discrete random variable with N possible values $\{1 \ldots N\}$, and T is the total number of observations. The hidden Markov chain defined by $P(Q_t|Q_{t-1})$, is represented by a stochastic transition matrix $\boldsymbol{A} = \{a_{i,j}\} = P(Q_t = j|Q_{t-1} = i)$. The special case of time $t = 1$ is described by the initial-state distribution $\pi_i = P(Q_1 = i)$. A particular sequence of observations O is represented as $O = (O_1 = o_1, ..., O_T = o_T)$. The probability that a particular observation vector occurs at a particular time t for a state j is $b_j(o_t) = P(O_t = o_t|Q_t = j)$. The set of parameters is described as $\lambda = (\boldsymbol{A}, \{\boldsymbol{b_j(\cdot)}\}, \pi)$.

Three basic problems are to be solved for an HMM:

1. Find $P(O|\lambda)$ for some $O = (o_1, \ldots, o_T)$.
2. Given some O and λ, find the best state sequence $q = (q_1, \ldots, q_T)$ that explains O.
3. Find λ that maximizes $P(O|\lambda)$.

A maximum-likelihood method of parameter-estimation to find the parameters of an HMM has been proposed in reference [3]. In this study, we model the transitions between *segments* using an HMM.

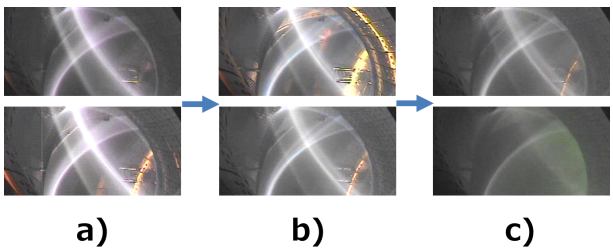

Fig. 1 Examples of *segments*.

4. Proposed Methods

4.1 Feature values

Four types of feature values are adopted: *color*, the amount of brightness transition (ABT), the speed of brightness transition (SBT), and the *shape*. These are defined by Eqs. (3) - (6), respectively.

$$Color(R, G, B) = \frac{1}{|\boldsymbol{F}|} \sum_{\boldsymbol{r} \in \boldsymbol{F}} |f(\boldsymbol{r})|. \quad (3)$$

$$ABT = bright_t - bright_{t-1}. \quad (4)$$

$$SBT = \frac{bright_t - bright_{t-1}}{seg\_num}. \quad (5)$$

$$Shape = \frac{4\pi \times area}{circumference^2}. \quad (6)$$

Here, $f(\boldsymbol{r})$ is the pixel value at the coordinate $\boldsymbol{r}$ of the first frame of a *segment*. The quantity $\boldsymbol{F}$ is the sum of all pixels in the first frame of a *segment*. We calculate the three *colors* red, blue, and green. The quantity $bright_t$ is the mean luminance value of the first frame of the t^{th} *segment*, seg_num is the number of frames in the $(t-1)^{th}$ *segment*, $area$ is the total value of the brighter pixels after binarizing the frame, and the $circumference$ is the peripheral length of the bright part after binarization. In the present study,

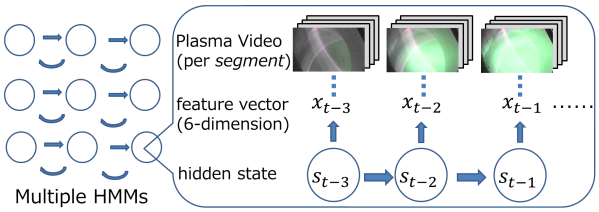

Fig. 2 The model generated from a plasma video.

for each *segment*, six-dimensional features are used, and the feature values are calculated for each *segment*.

4.2 Plasma-emission model from an HMM

We model the transitions between *segments* in similar videos based on an HMM, and term the resulting model as the "plasma-emission model." Figure 2 outlines a plasma emission model. The feature vector of a *segment* is regarded as an observation vector o_t, and a transition between *segments* is represented by a transition between hidden states Q_t. The observation vectors are continuous; therefore, the probability distribution $P(o_t|Q_t)$ is assumed to be a mixture of multivariate Gaussians for each state.

4.3 Selection of similar videos

An HMM can determine the best state sequence q. The plasma videos can be converted into a symbol series, which represents the series of hidden states $q = (q_1, \ldots, q_T)$. Here, two or more plasma videos are assumed to be similar when their symbol series are the same because the symbol series represent a time-series pattern. In this study, we used half of the prepared videos to train the HMM and employed the other half to test the trained HMM. For some videos, the videos are determined to be similar if three or more symbol series were the same; this number was determined experimentally. For example, assuming that the symbol series for video S is (A, B, B, C, D) and that for video T is (E, A, B, B, C, A), videos S and T are similar because four symbol series (A, B, B, C) are the same. In this way, the prepared videos are categorized into several groups. We can then train the HMMs using similar videos and obtain multiple models that represent the plasma-emission pattern for each similar video. This procedure is shown in Fig. 3.

4.4 Evaluation of the optimal model

An optimal plasma-emission model can be selected from the models obtained from a new video. Using the Viterbi algorithm [3], for each plasma-emission model, the t^{th} state q_t for the t^{th} *segment* of a new video can be determined.

We can calculate the Euclidean distance between the mean parameters $\boldsymbol{\mu} = (\mu_1, \ldots, \mu_6)$ for the t^{th} state of a plasma-emission model q_t and the feature vector $o_t = (v_1, \ldots, v_6)$ for the t^{th} *segment* of a new video. This Euclidean distance is represented as $dis_j(t)$ $(j = 0, \ldots, 22)$ for

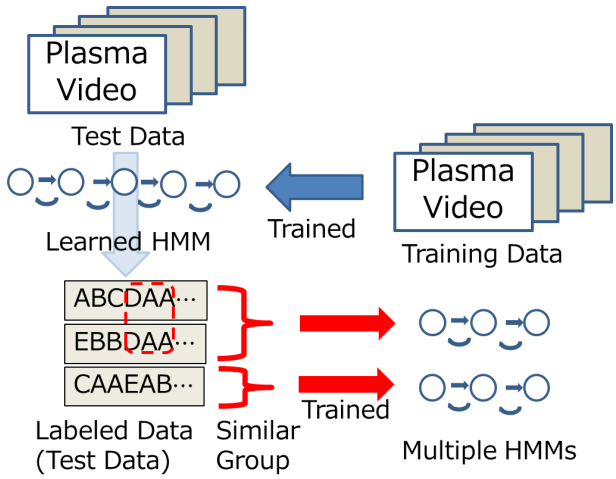

Fig. 3 Generation of multiple models.

the plasma-emission $model_j$. When the values of $dis_j(t)$ are arranged in ascending order, the ordered distance is denoted by $Dis_{j,t}(k)$, where k is the order after sorting. For example, consider a case in which $model_3$ is the second similar plasma-emission model to the 4^{th} *segment* of a new video. In this case, $dis_3(4)$ is the Euclidean distance between the mean parameters of the fourth state of the third plasma-emission model and the feature vector of the fourth *segment*, and $Dis_{3,4}(2)$ is the second distance among these ordered values.

Let us consider the point at which the distance $Dis_{j',t}(k+1) - Dis_{j,t}(k)$ becomes larger than the previous value $Dis_{j,t}(k) - Dis_{j'',t}(k-1)$. We label this point as N_t. The state q_t and the feature vector o_t are regarded as similar up to N_t. The top N_t^{th} plasma-emission models are then considered to be optimal for the t^{th} *segment* of the new video.

For each *segment*, we calculate the value of N_t. For each plasma-emission model, the *number of selections as the top* N_t^{th} *models* (NST) is incremented according to the *segment* number t. The value of NST is considered to represent the similarity of the plasma-emission model to the new video. Figure 4 shows an example of the method for calculating NST. In this example because Models A and B are selected as the top N_t^{th} plasma-emission models at time t, the NSTs of Models A and B are incremented. The same process is repeated for successive time increments. In this case, Model A is the most similar to the example plasma video because NST of Model A is the largest.

4.5 Determining the next emission

The transition probability can be obtained for each state; hence, the probable next state can be estimated from the current state. The symbol series are obtained from the plasma video used in the HMM; therefore, by obtaining the symbol series for the *segment* data used to train the plasma-emission model, it is possible to detect the types of *segments* that each state of the plasma-emission model

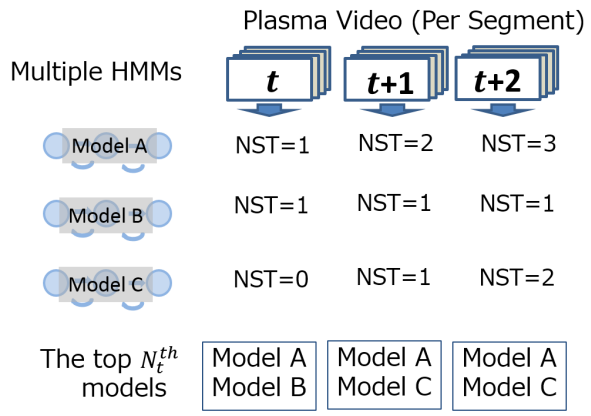

Fig. 4 Method to calculate NST.

is composed of. The first frame of this *segment* is used as the representative frame for the *segment*, and is used in the visualization of each state of the plasma-emission model.

5. Experiment

5.1 Experimental method

We prepared 148 videos, which we grouped into 23 plasma-emission models ($model_0$-$model_{22}$). We also prepared three test videos (t1 to t3) to evaluate the proposed method.

We evaluated the plasma-emission model from two perspectives: 1) Has the appropriate plasma-emission model been selected for the test video from among multiple models? 2) Does the plasma-emission model appropriately predict future plasma emissions?

For each test video, we calculated the value of NST for each plasma emission model. Next, we compared the test video and the videos used in creating plasma models with an NST larger than unity. Next, we selected a plasma-emission model similar to the test video ($Model_{sim}$). This model was used to evaluate the response to perspective (1). Subsequently, we used $Model_{sim}$ to predict a candidate for the probable next state to evaluate the response to perspective(2).

5.2 Evaluation methods

We then examined where $Model_{sim}$ is ranked in NST for each *segment*. We also evaluated the ratio of the number of *segments* that include correct candidate images predicted in the top 80% of transition probability ($Num_{correct}$) to the total number of *segments* (Num_{seg}). The value obtained by dividing $Num_{correct}$ by Num_{seg} is called the "ratio of prediction" (RP), and is defined by Eq. (7).

$$RP = \frac{Num_{correct}}{Num_{seg}}. \tag{7}$$

5.3 Results

Figure 5 shows the values of NST for test videos t1 and t2 obtained through the method described above. The

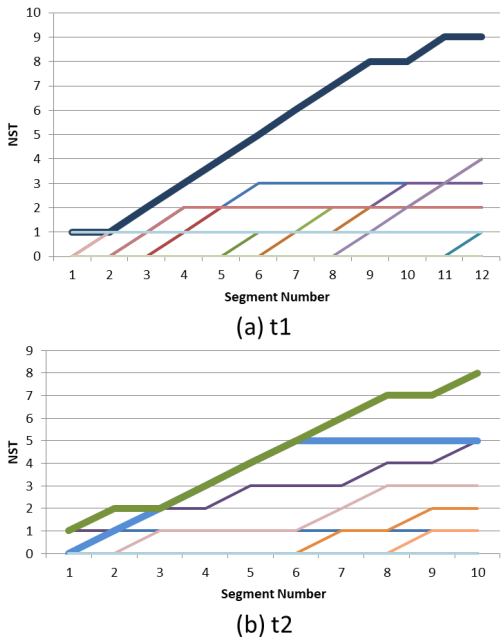

Fig. 5 Transitions of NST per *segment*. Each colored line represents a specific plasma-emission model. The bold lines are $Model_{sim}$, which adopts large values as compared with the thin lines.

Table 1 Mean Rank of $Model_{sim}$.

Video	Mean Rank	Number of *segments*	RP
t1	1.00	12	0.58
t2-1	1.00	10	0.20
t2-2	1.56	10	0.09
t3	2.10	11	0.09

vertical axis is NST, and the horizontal axis is the time in a *segment*. The bold lines show $Model_{sim}$, and the thin colored lines show other models. Each color represents a different model. The mean rank of $Model_{sim}$ among all 23 models is shown in Table 1, together with the corresponding value of RP.

As shown in Fig. 5, $Model_{sim}$ is selected as an optimal model, rather than the other models; in the later *segments* in particular, $Model_{sim}$ has a higher value of NST. For test video t2, two versions of $Model_{sim}$ exist: t2-1 and t2-2. According to Table 1, the RP values are different for these test viedos. The mean rank of $Model_{sim}$ is 1.42. This shows that the proposed method is effective in selecting the optimal model, even though the performance of the models is different.

Examples of the first frames of *segments* and the sequence of the symbol series for t1 and t2 are shown in Figs. 6 and 7, respectively. Examples of plasma-emission-model parameters are shown in Tables 2 and 4, respectively, while the mean parameters are shown in Tables 3 and 5, respectively. All mean values are normalized.

From Fig. 6, it can be seen that emissions of similar colors correspond to the same hidden state. Table 2 shows

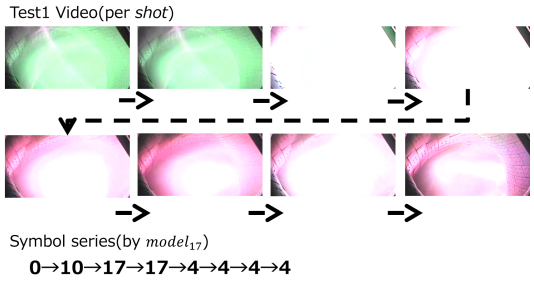

Fig. 6 Test video t1 and the corresponding symbol series.

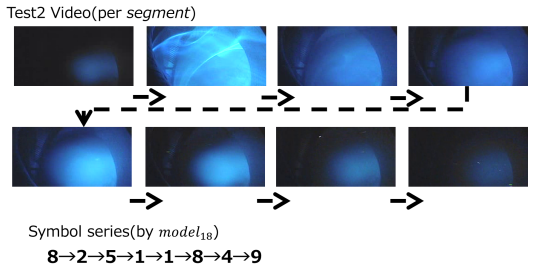

Fig. 7 Test video t2 and the corresponding symbol series.

Table 2 Example of Plasma-Emission Transition ($model_{17}$).

State ID	Features	Transition Probability	Transition Destination
0	Green, Bright	0.56	10
		0.22	17
		0.11	0
		0.11	7
4	Red, Bright	0.50	4
		0.50	15
10	Green, Bright	0.50	10
		0.30	0
		0.10	7
17	White, Bright	0.50	17
		0.17	4
		0.17	5
		0.17	8

Table 3 Mean Parameters of Plasma-Emission $model_{17}$.

State ID	B	G	R	ABT	SBT	Shape
0	1.10	1.68	1.03	0.23	0.40	0.74
4	1.10	0.65	1.61	-0.88	-1.01	0.50
10	0.93	1.58	0.87	-1.04	0.03	0.76
17	1.80	1.96	1.72	0.34	0.53	0.82

that the probability of transitioning from one bright emission to another is high. For example, the probability of a transition from State ID 17 to 17 is high.

Figure 7 shows that even if the colors are the same, many *segments* can be decoded to different states. Table 4 shows that visually, many states have the same color.

Table 4 Example of Plasma-Emission Transition ($model_{18}$).

State ID	Features	Transition Probability	Transition Destination
1	Blue, Bright	0.25	1
		0.75	8
2	Blue, Bright	1.00	5
4	Blue, Dark	0.67	6
		0.33	9
5	Blue, Bright	0.75	1
		0.25	5
8	Blue, A Little Bright	0.25	2
		0.75	4

Table 5 Mean Parameters of Plasma-Emission $model_{18}$.

State ID	B	G	R	ABT	SBT	Shape
1	0.84	0.32	-0.84	-0.46	-0.06	1.06
2	1.37	0.58	-0.79	1.18	1.73	0.98
4	-0.57	-0.83	-1.09	-0.69	-0.75	1.11
5	1.49	0.85	-0.65	0.16	0.29	0.99
8	0.25	-0.31	-0.96	-0.51	-0.52	1.11

6. Discussion

According to Fig. 5, the differences among the values of NST are not large at the beginning of a video, but the value of NST for the bold line gradually increases more than those of the thin lines in the later *segments* because a similar video has more similar *segments* than non-similar ones.

In test video t1, the plasma emissions are green, red, and white, and the duration of the bright emission is relatively longer than that for the other test videos. Hence, the *segments* from this video seem to be special. We can actually observe the differences in the *segments* visually. Conversely, in test video t2, the plasma emission is dark, and hence, visually selecting similar *segments* is difficult. In Table 1, the mean RP is low. This indicates that many predicted images were different from the actual images. However, as RP is not 0 it can be seen that the image that is appropriately predicted was included in the prediction candidates.

We consider that the difference in the mean rank of each video and the value of RP are due to the pattern of the plasma emission.

7. Conclusion

In this study, we proposed a method for estimating plasma-emission transitions using an HMM trained on plasma-emission videos.

We also proposed a plasma-emission model and a method for selecting similar videos. We selected the models using an HMM and confirmed that the plasma videos

are well-classified. We conducted an evaluation experiment using the model rank results and showed that the optimal model has a higher rank than others. We also conducted that acquiring knowledge about plasma emissions using the hidden Markov model is possible.

We plan future studies to improve this model and make it more robust to various emission patterns.

Acknowledgment

This research is partly supported by the National Institute for Fusion Science under NIFS15KLEH046.

[1] Large Helical Device Project Home Page, http://www.lhd.nifs.ac.jp/ (reference 12-21-2017).

[2] M. Shoji, K. Yamazaki and S. Yamaguchi, "Development of the Real-time lmage Data Acquisition System for Observing the Plasma Dynamic Behavior of LHD Long-pulse Discharges", J. Plasma Fusion Res. SERIES **3**, 440 (2000).

[3] J. Bilmes, "A gentle tutorial on the EM algorithm and its application to parameter estimation for Gaussian mixture and hidden markov models" (Technical Report ICSI-TR-97-02, University of Berkeley, 1997).

[4] H. Woo, Y. Ji, H. Kono and Y. Tamura, "Estimation Method for Lane Changes of Other Traffic Participants Using State-Unit based Hidden Markov Models", Robotics Symposia proceedings **21**, 222 (2016).

[5] H. Ohya and S. Morishima, "Automatic Music Video Generating System by Learning Existing Contents Based on Hidden Markov Model", Music and computer (MUS) Technical Report **2012-MUS-95**, 1 (2012).

[6] H. Shiroshita, T. Hochin, H. Nomiya and H. Nakanishi, "Similarity Retrieval of Plasma Videos and Its Evaluation", Proc. of 3rd Int'l Conf. on Applied Comp. and Inf. Tech. (ACIT 2015), 229 (2015).

[7] H. Shiroshita, T. Hochin, H. Nomiya and H. Nakanishi, "Revised Similarity Retrieval Method of Plasma Emission Videos and Its Evaluation", Proc. of 18th IEEE/ACIS Int'l Conf. on Softw. Eng., Artif. Intell., Networking and Parallel/Distr. Comp. (SNPD 2017), 575 (2017).

[8] Y. Chida, H. Koga and T. Watanabe, "Fast Detection of Query Videos from Video Streams" (DEIM Forum 2013 D1-5, 2013).